NUMERICAL APPROACH TO THE MECHANICS OF DISC-BLADE DOVETAIL JOINTS IN AERO-ENGINE COMPRESSORS

M. M. I. Hammouda[1] and A. S. Fayed[2]
[1] Mechanical Engineering Department, Al Azhar University, Egypt
[2] Materials Engineering Department, Zagazig University, Egypt

ABSTRACT

In this paper the macro mechanics behaviour of the fretted surfaces in dovetail joints between blades and discs in aero-engine compressors is numerically analysed. Two-dimensional elastic-plastic finite element analysis simulates incremental loading conditions during normal engine operational cycles. One simulated cycle includes the modes of disc acceleration, full blade loading and unloading and final deceleration. Results are obtained from two of such cycles. Computation marching is based on the detection of the earliest candidate out of possible contact and elastic-plastic events at each increment.

The edges of the common surfaces nearest to the dovetail notch base are justifiably the sites of the initiation of fatigue failure of the disc and the blade. The present results correspond to a friction coefficient of 0.25.

1 INTRODUCTION

Dovetail roots are used to fix the blades on the discs for the fan assembly and in the low pressure stages of rotating compressors in turbines used for aircraft propulsion. Fretting fatigue problems have been reported in these joints [1]. The resulting bulk stress and contact pressure between the disc and the blade root together with the relative displacements are responsible for the fretting fatigue phenomena. The failure of the joint could be catastrophic and the possibility of its occurrence necessitates modifications leading to economical losses. An accurate analysis is paramount to scientifically approach the challenge confronting the designers of aero-engines. To avoid relatively expensive full scale tests, numerical and experimental trials were made to simulate loaded disc-blades assembly [2]. Tensile tests of simplified dovetail blades inserted into simplified fan disc models and attempts of small-scale biaxial fatigue tests were carried out. Numerically, commercial finite element (FE) codes were utilized to analyze the behavior of dovetail joints with different friction coefficients [3]. Contact elements were used at the common surfaces of a single sector representing the disc. These idealizations used loads not matching the loading met during normal engine operations. Only monotonic centrifugal forces were considered and collectively applied at the blade end. The boundary conditions along the radial borders between the analyzed sector and the remaining part of the original disc were neither considered nor correctly formulated [3-4]. Obviously, the continuity of the whole disc was not preserved in this case.

The normal engine operational cycle consists of starting and warming up, rise to full power, reduction to cruising conditions, idling prior to landing, and a power surge on landing before final engine shutdown. In addition, fluid flow round the blades may cause their vibration at high frequencies. Consequently, high levels of both centrifugal forces and pressures are cyclically applied on the assembly during the engine operation. This paper presents FE treatment of dovetail joints in aero-engine compressors during normal engine operational cycles.

2 PROBLEM DESCRIPTION

A disc-blades assembly of an aero-engine compressor is assumed mounted on a circular rotor. The blades are assembled into the disc with frictional dovetail joints. The disc is divided into identical sectors each accommodates a blade. The sector is initially symmetrical about the horizontal axis,

see Fig. 1(a). The disc is assumed rotating in a clockwise direction. Inertia forces are distributed all over the assembly. The sector is externally subject to forces acting at its common surface with the rotor, its two outer radial borders and the blade surface. Coulomb friction is assumed. Appropriate boundary conditions are devised to preserve the continuity of the whole disc with the analysis of the sector. Elastic-plastic FE package is utilised [5]. The von-Mises yield criterion and the Prandtl-Reuss flow rule are adopted. The Prager-Ziegler kinematic hardening model is employed. In the plastic regime, a simple power stress-strain law is used.

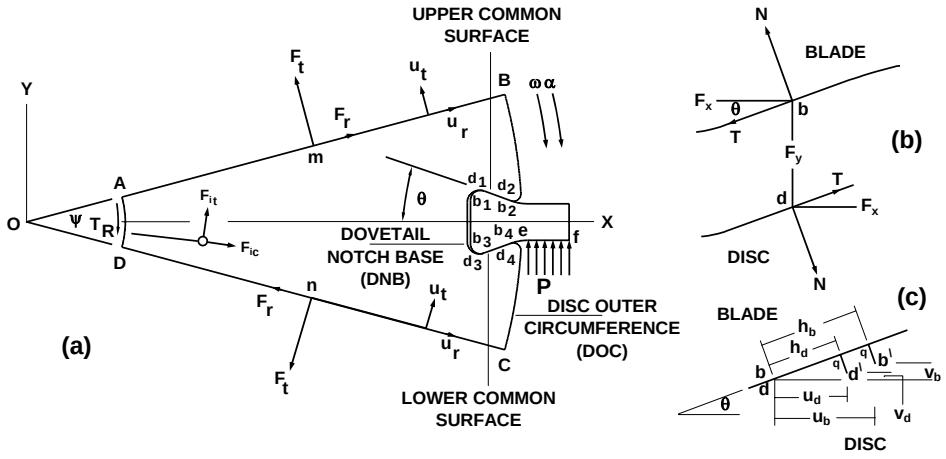

Fig. 1 Present idealization (a) a single sector with the boundary conditions, (b) forces mutually acting on a contact pair and (c) displacements of a contact sliding pair

3 PRESENT SOLUTION

After the application of the boundary conditions, a system of algebraic equations is generated which are not ready to be directly solved. In this form, an iterative procedure is unavoidable to have the displacement and internal force fields within the assembly. The present solution adopts the previously published mathematical treatment [5] purposely devised to manipulate the stiffness matrix with no need of such iteration. The analysis starts with the disc appropriately supported, initially un-deformed and having all the contact pairs along the straight common surfaces assumed sticking. The schematic of Fig. 2(a) shows a loading cycle. The first increment of the acceleration mode is marched to have the corresponding incremental inertia forces applied.

The problem is solved for the displacement field and the internal forces acting at the nodal points along the common surfaces. The relevant kinematic and kinetic data given by the resulting solution are used to update the contact regime of each pair. The new contact data are induced to the boundary conditions of the problem to compute a new corresponding solution. Such an iterative procedure is terminated when the resulting contact regimes do not violate any of the basic concepts outlined before. A new time increment is successively allowed until the maximum disc speed is reached. During the acceleration and deceleration modes the variation of the disc angular speed and acceleration with time are assumed sinusoidal. Similarly, the blade is incrementally loaded until maximum pressure is achieved. Incremental unloading, loading and unloading follow. The disc is, then, incrementally decelerated until it stops. Further cycles can, then, be applied.

During an increment step, possible events are recognised as (1) the change in regime of a contact pair, (2) the change in the elastic-plastic regime of an element and (3) the achievement of any of the next maximum or zero value of the speed, acceleration and the load within the loading

cycle. The candidates susceptible to the application of each event are identified. A minimum scale factor is computed for the occurrence of an event within its candidates. Such minimum values are utilised to recognise which event is to take place first and the corresponding scale factor which decides the current increment. Having that factor known, all the initial parameters necessary as inputs for the next step can be computed. Thus, deformation, internal force and stress-strain fields generated within the system are continuously traced during the operational cycle.

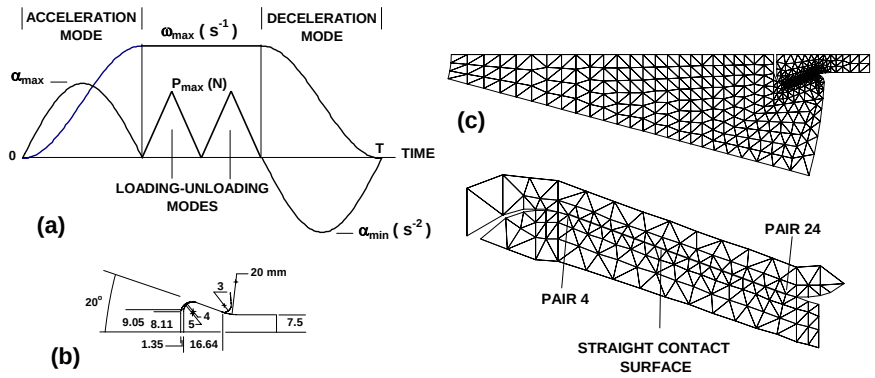

Fig. 2 Present application (a) simulated loading conditions during, (b) dimensions of the joint and (c) Half of the analysed mesh

4 PRESENT APPLICATION

The analysis was applied on the disc and blade geometries [4] shown in Fig. 2(c). The geometry corresponds to the compressor disc of the aeroengine RB211 used in Jumbo jets. Fig. 2(c) shows the geometry of half of the full domain of the idealised sector. Each disc/blade common surface had 24 equally spaced contact pairs. The plane strain analysis was assumed. The material properties modeled for the blade and the disc were those of titanium alloy Ti-6Al-4V [4]. The modulus of elasticity, the Poisson's ratio, the yield stress, the strain hardening exponent and the density were respectively 114 GPa, 0.33, 1100 MPa, 0.2 and 4429 kg/m^3. The present results correspond to a relatively low value of μ between the fretting surfaces, = 0.25. The behaviour of the system was simulated for a maximum disc speed of 12000 rpm, a full blade load of 4000 N and an acceleration/deceleration time of 6 minumtes. Two operational cycles were simulated.

5 RESULTS AND DISCUSSION

Based on the balances of forces , torques and energy involved within the present problem, the error percentages for each computational step indicated a maximum value of 1.5%. This proved that the present problem had been properly formulated. Table 1 presents information relevant to the contact development along the contact surfaces during a loading mode and locally during the different loading modes. This table is constructed from a knowledge of (1) the devoplment of the relative tangential displacement of the two nodes constituting the pairs along the straight common surfaces of the joint during the simulated two operational cycles is one form of the output of the present analysis and (2) the corresponding contact forces. As a result of loading change, the events of separation, sliding contact and sticking contact are exchanged along the two straight flanks of the joint. The existence of more than one letter within a zone indicates a transition from a contact regime to another within the same loading mode. A single letter within a zone means an immediate change when the load mode changes. Separation and closure are invariably developed in

sequences. Closure takes place with the reverse order of the last separation process. Separation starts at the latest closed pair and continues in the reverse order of the last closure process. A pair slides before its separation. A separated pair starts its contact sliding.

On accelerating the disc, the lower common surface (LCS) is being displaced downwards with a clockwise rotation. During that mode continuous upward displacement with an anticlockwise rotation is experienced by the upper common surface (UCS). During the blade loading, both common surfaces are being upwardly displaced with an anticlockwise rotation. The displacement and rotation of both common surfaces are reversed during the blade unloading. The variation in normal displacement and rotation of the common surfaces during the first and the next loading-unloading modes are similar. When the deceleration of the disc is terminated the blade approximately recovers its original position with a slight upward displacement. Due to the application of the second cycle the two common surfaces behave as previously described.

At a specified disc speed, ω, during the disc acceleration mode, the pressure, N, continuously decreases along the two common surfaces from a maximum value at the contact edge nearest to the dovetail notch base (DNB), i.e. pair 4, to a minimum value at the contact edge nearest to the disc outer circumference (DOC), i.e. pair 24. As ω increases, N increases along the contact surfaces. The distribution of N along the two surfaces is the same during that mode for the inertia forces due to tangential acceleration is extremely small relative to the corresponding centrifugal forces. On the next blade loading, N acting on the pairs of the LCS neighbouring to the separated pairs continuosly decreases with a simultaneous increase in N acting on the pairs nearest to the DNB towards which the corresponding resultant, Σ_{LCS}, is shifted. During that loading mode, N acting on pair 24 of the UCS and its neighbouring pairs continuously increases with a decrease in N acting on pair 4 and its neighbouring pairs. At maximum load, a uniform normal force distribution is formd along a wide middle part of the UCS and two peak N values exist at its two edges with a higher value acting on pair 24. The corresponding resultant, Σ_{UCS}, is shifted towards the DOC. Due to blade loading, $\Sigma_{UCS} > \Sigma_{LCS}$. During the next unloading mode there is a continuous decrease in N acting on the pairs along the LCS neighbouring to the DNB and an increase in N acting on the pairs neighbouring to the open zone. With respect to the UCS, N acting on the pairs nearest to the DOC continuously decreases on unloading whilst N acting on the pairs nearest to the DNB increases. That ends with two peak values of N acting on the two edges of the UCS with a higher value at pair 4. Along both common surfaces, the sequence of changing N during the latter unloading is reversed during the next blade loading and repeated during the second blade unloading. Early on decelerating the disc, the value of N acting on the pairs along the LCS neighbouring to the separated zone increases whilst the pairs on the other side of its flank decreases. Beyond the closure of the open pairs on the LCS the value of N acting on its pairs decreases with different rates as the disc speed decreases. During that mode, the value of N acting on the pairs along the UCS continuously decreases with decreasing ω. At the termination of that mode, all the pairs are separated. The above development of the normal force is approximately repeated in the course of the second simulated operational cycle.

As demonstrated in Table 1, all the contact pairs on both common surfaces cyclically slip. For most of the pairs, a cycle results in outward and inward sliding of the blade relative to the disc. Entire outward sliding starts on accelerating the disc. Sliding is terminated at the end of acceleration for the UCS and at the end of the next loading mode for the LCS. Inward sliding is a result of decelerating the disc. The LCS experiences more range of cyclic slipping than the UCS. The hysetresis loops for the contact pairs along the common surfaces plotted as tangential contact force against its corresponding relative sliding displacement during the simulated cycles are generated. This indicates that pair 4 on the LCS is the most susceptible site to wear.

Table 1
Contact development along the common surfaces during the two simulated cycles

Pairs on the Straight Flank of the Lower Contact Surface

	4-8	9-14	15-19	20-23	24
Acceleration	R				
Loading	R		RO		
Unloading	RC	RL\	OL\	O	
Loading	CR\	L\R\	L\R\O	O	
Unloading	R\C	R\L\	OL\	O	
Deceleration	CLO	L\LO		OLO	
Acceleration	OR				O
Loading	R		RO		O
Unloading	RC	RL\	OL\	O	
Loading	CR\	L\R\	L\R\O	O	
Unloading	R\C	R\L\	OL\	O	
Deceleration	CLO	L\LO		OLO	

Pairs on the Straight Flank of the Upper Contact Surface

	4-8	9	10	11	12-16	17-21	22-24
Acceleration	R						
Loading	C		CL\				
Unloading	CR\	C	L\C				L\CR\
Loading	R\C	C				CL\	R\CL\
Unloading	CR\	C				L\C	L\CR\
Deceleration	R\LO	CLO					R\LO
Acceleration	OR						
Loading	C		CL\				
Unloading	CR\	C	L\C				L\CR\
Loading	R\C	C			CL\		R\CL\
Unloading	CR\	C			L\C		L\CR\
Deceleration	R\LO	CLO					R\LO

O	Open
C	Sticking
R	The blade node is sliding relative to the disc nodealong the outward direction
L	The blade node is sliding relative to the disc node along the inward direction
R\	Sticking with the blade node impending to slide relative to the disc node along the outward direction
L\	Sticking with the blade node impending to slide relative to the disc node along the inward direction

Figure 3 demonstrates plasticity development during the simulated cycles. Plastically deformed elements invariably exist neighbouring to joint edges nearest to the DNB and the DOC. Seven elements are plastically deformed on the disc side either during loading and unloading of the blade or during the disc deceleration. Two blade elements are plastically deformed only during the first loading. The above nine elements are possible sites of fatigue crack initiation (FCI). One of the initiated cracks will be dominant and lead to failure either of the disc or of the blade. Biaxial non-proportional stress-strain fields are generated. To expect the crack leading to final failure, more analysis of those fields is needed. One vertix of the element 517 is the disc node of pair 4 which lies on the LCS straight flank. This is the area which is most susceptible to wear. Element 564 is not located on a common surface and can be a subsurface site of FCI. The three elements 6, 7 and 648 are elastically deformed during the second cycle. The behavior of those elements is not expected to change due to the application of further cycles. However, in the case of a relatively higher loading, any of those element may be operative. Element 6 is a candidate as FCI site in the blade material. The two elements 688 and 642 lie along the UCS curved flank and they are not directly affected by fretting . However, frictional forces existing along the joint common surfaces affect their near stress field. Similarly, element 515 belongs to the area just neighbouring to the LCS straight flank on the disc. Element 518 is the next neighbour of element 517. Further, for the two elements 688 and 642 the normal strain, ε_n, acting on the plane of maximum shear strain is invariably positive during the simulated cycles. For the other seven elements, ε_n is always negative. Crack initiation near the edge of the straight common surface has been reported by other

researchers [4]. The principal planes corresponding to each element continuously rotate. Again, the prediction of the initiated crack angle needs more analysis.

5 CONCLUSIONS

A finite element package has been successfully developed to simulate the macro mechanics behaviour of the fretted surfaces in dovetail joints between blades and discs in aero-engine compressors with normal operational loading cycles. Boundary conditions have been appropriately tailored for the problem. The following conclusions correspond to a friction coefficient of 0.25.

1. The edges of the common surfaces nearest to the dovetail notch base are justifiably the sites of the initiation of fatigue failure of the disc and the blade.
2. During an engine operation, continuous changes along the common surfaces occur in the contact regimes, the distribution of the normal and tangential internal reactions, the relative normal and tangential displacements, the sites of plastic deformation and the direction of principal planes.

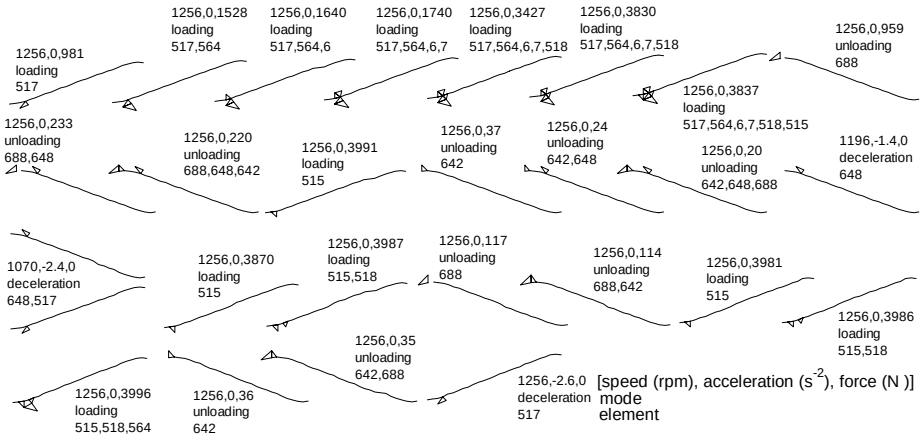

Fig. 3 Plasticity development during the two operational cycles

REFERENCES

1. N. S. Xi, P. D. Zhong, H. Q. Huang, H. Yan and C. H. Tao (2000) Failure investigation of blade and disk in first stage compressor. Engng Failure Analysis, 7, 385–392.

2. C. Ruiz and D. Nowell (2000) Designing against fretting fatigue in aero-engines. Fracture mechanics, applications and challenges, ECF 13, ESIS publication 26. Elsevier, 73–95.

3. R. L. Burguete and E. A. Patterson (1998) The effect of friction on crack propagation in the dovetail fixings of compressor discs. Proc Instn Mech Engrs, 212 Part C, 171-181.

4. S. A. Meguid (2000) On the mechanical integrity of aeroengine compressor disc assemblies. Current Advances in Mechanical Design and Production, Proc. Seventh Cairo University International MDP Conference, February 2000, 161-172.

5. M. M. I. Hammouda, H. E. M. Sallam and A. S. Fayed (2002) Mode II stress intensity factors numerically computed for central slant cracks with rough surfaces in uniaxially compressed plates. Int. J. Fatigue, 12, 1213-1222.

6. M. M. I. Hammouda, I. G. El-Batanony and H. E. M. Sallam (2003) Finite element simulation of the mechanics of flat contact pad fretting fatigue tests. Fatigue Fract Engng Mater Struct, 26, 1-13.